

Supporting Information for:

**Competitive Oxygen-18 Kinetic Isotope Effects Expose O–O
Bond Formation in Water Oxidation Catalysis by Monomeric
and Dimeric Ruthenium Complexes**

Alfredo M. Angeles-Boza,^{1,#} Mehmed Zahid Ertem,^{2,§} Rupam Sarma,¹ Christian H. Ibañez,¹
Somnath Maji,³ Antoni Llobet*,³ Christopher J. Cramer² Justine P. Roth*,¹*

¹Department of Chemistry, Johns Hopkins University, 3400 North Charles Street, Baltimore,
MD 21218

²Department of Chemistry and Research Computing Center, University of Minnesota, 207
Pleasant St. SE, Minneapolis, MN 55410

³Institute of Chemical Research of Catalonia (ICIQ), Av. Països Catalans, 16, 43007 Tarragona,
Spain

Table of contents	Page #
Full list of authors for Reference 35.	S-4
Calculations of ^{18}O isotope effects	S-4
Table S-1. Reduced partition function calculation of ^{18}O KIE(O–O) for Ru .	S-11
Table S-2. Reduced partition function calculation of ^{18}O KIE(O–O) for Ru₂^{BD} .	S-12
Table S-3. Reduced partition function calculation of ^{18}O KIE(O–O) for Ru₂^{Hbpp} .	S-13
Calculated vibrational frequencies for water	S-15
Table S-4. Reduced partition function calculation of ^{18}O KIE(H ₂ O) for Ru .	S-16
Table S-5. Reduced partition function calculation of ^{18}O KIE(H ₂ O) for Ru₂^{BD} .	S-17
Table S-6. Reduced partition function calculation of ^{18}O KIE(H ₂ O) for Ru₂^{Hbpp} .	S-19
Additional computational analysis	S-20
Table S-7. Summary of DFT calculated parameters for catalysis by Ru .	S-21
Table S-8. Summary of DFT calculated parameters for catalysis by Ru₂^{BD} .	S-22
Table S-9. Summary of DFT calculated parameters for catalysis by Ru₂^{Hbpp} .	S-23

Table S-10: Comparison of gas phase ^{18}O KIE(H_2O) and ^{18}O KIE(D_2O)	S-24
Figure S-1: UV-Vis Spectrum and Beer's Law Plot for Ru_2^{BD} .	S-25
Figure S-2: Quantitative ^1H -NMR spectrum of Ru_2^{BD} .	S-26
Figure S-3: Expanded views of the spectrum in Figure S-2.	S-27
Figure S-4: UV-Vis Spectrum and Beer's Law Plot for Ru .	S-28
Figure S-5: Quantitative ^1H -NMR spectrum of Ru .	S-29
Figure S-6: UV-Vis spectrum and Beer's Law plot for $\text{Ru}_2^{\text{HbPP}}$.	S-30
Figure S-7: Quantitative ^1H -NMR spectrum of $\text{Ru}_2^{\text{HbPP}}$.	S-31
Figure S-8: Plots of initial rate versus Ru (a), Ru_2^{BD} (b) and $\text{Ru}_2^{\text{HbPP}}$ (c)	S-32

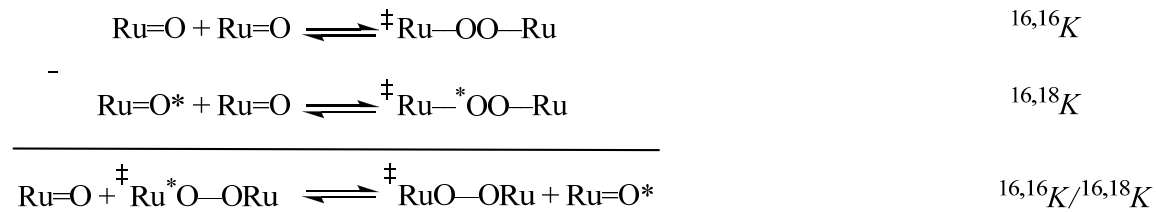
Full Lists of Authors for (Gaussian) Reference 35b.

Gaussian 03, Revision C.02, Frisch, M. J.; Trucks, G. W.; Schlegel, H. B.; Scuseria, G. E.; Robb, M. A.; Cheeseman, J. R.; Montgomery, Jr., J. A.; Vreven, T.; Kudin, K. N.; Burant, J. C.; Millam, J. M.; Iyengar, S. S.; Tomasi, J.; Barone, V.; Mennucci, B.; Cossi, M.; Scalmani, G.; Rega, N.; Petersson, G. A.; Nakatsuji, H.; Hada, M.; Ehara, M.; Toyota, K.; Fukuda, R.; Hasegawa, J.; Ishida, M.; Nakajima, T.; Honda, Y.; Kitao, O.; Nakai, H.; Klene, M.; Li, X.; Knox, J. E.; Hratchian, H. P.; Cross, J. B.; Adamo, C.; Jaramillo, J.; Gomperts, R.; Stratmann, R. E.; Yazyev, O.; Austin, A. J.; Cammi, R.; Pomelli, C.; Ochterski, J. W.; Ayala, P. Y.; Morokuma, K.; Voth, G. A.; Salvador, P.; Dannenberg, J. J.; Zakrzewski, V. G.; Dapprich, S.; Daniels, A. D.; Strain, M. C.; Farkas, O.; Malick, D. K.; Rabuck, A. D.; Raghavachari, K.; Foresman, J. B.; Ortiz, J. V.; Cui, Q.; Baboul, A. G.; Clifford, S.; Cioslowski, J.; Stefanov, B. B.; Liu, G.; Liashenko, A.; Piskorz, P.; Komaromi, I.; Martin, R. L.; Fox, D. J.; Keith, T.; Al-Laham, M. A.; Peng, C. Y.; Nanayakkara, A.; Challacombe, M.; Gill, P. M. W.; Johnson, B.; Chen, W.; Wong, M. W.; Gonzalez, C.; Pople, J. A. Gaussian, Inc., Wallingford CT, 2004

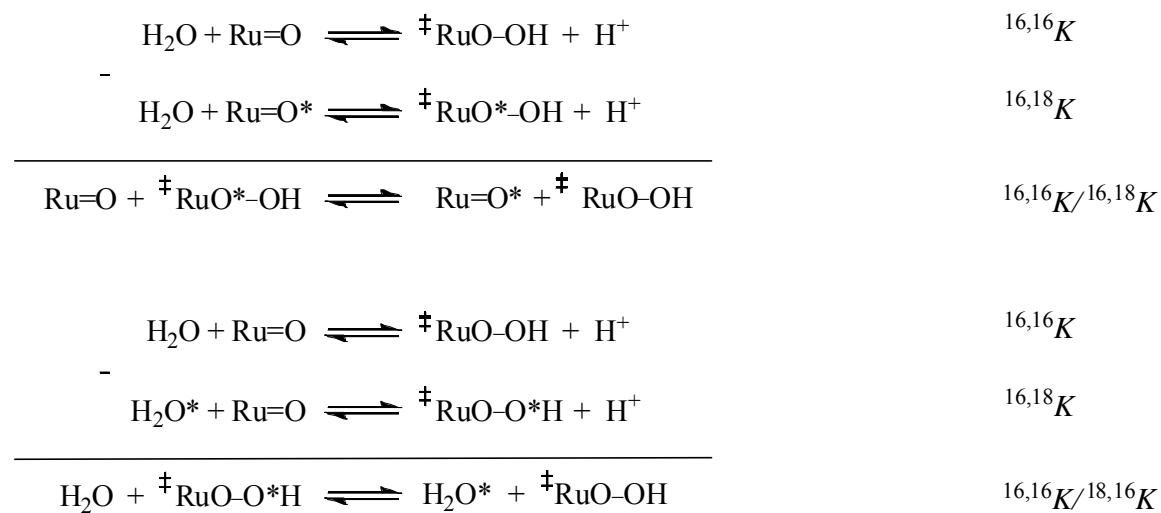
Calculations of ^{18}O EIEs and ^{18}O KIEs

Isotope exchange reactions (Schemes S1-S4) are used to define reduced partition function ratios for the computation of ^{18}O EIEs and ^{18}O KIEs are provided below. Each reactant and product of every step in the catalytic reactions mechanism is considered, following the approach outlined by Bigeleisen and Goepert-Mayer.

Scheme S1. The isotope exchange reaction used to define irreversible oxo-coupling (OC).

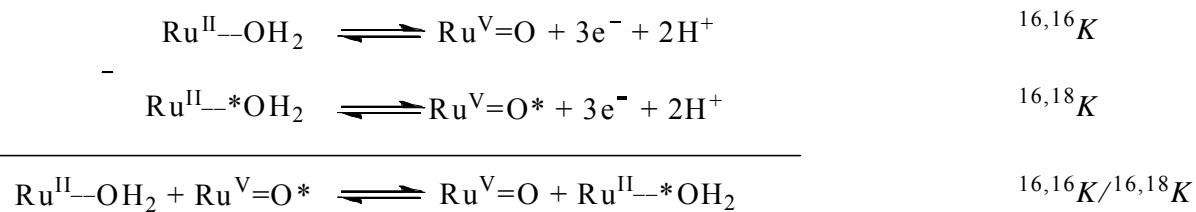


Scheme S2. Isotope exchange reactions used to define irreversible water attack (WA).

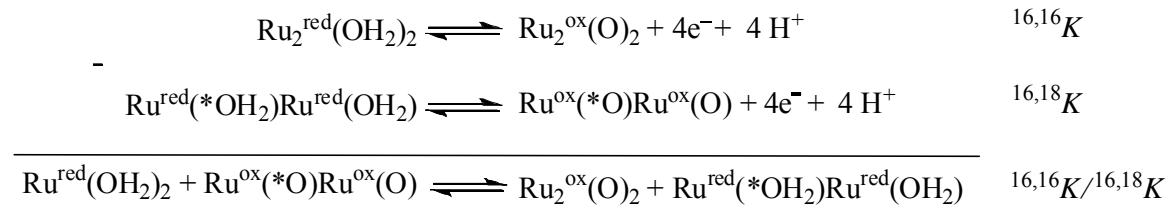


Scheme S3. Isotope exchange reactions for the oxidation of monomeric (a) and dimeric (b) ruthenium complexes.

(a)

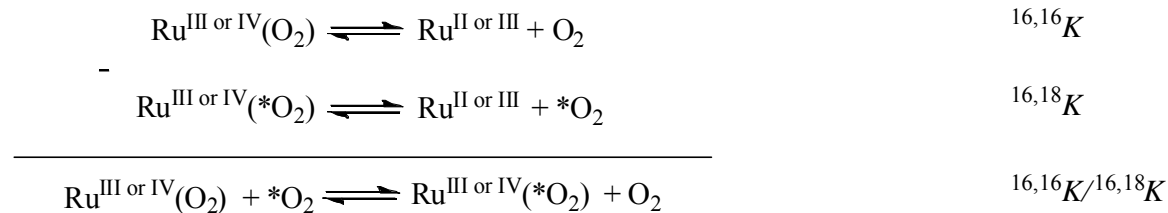


(b)

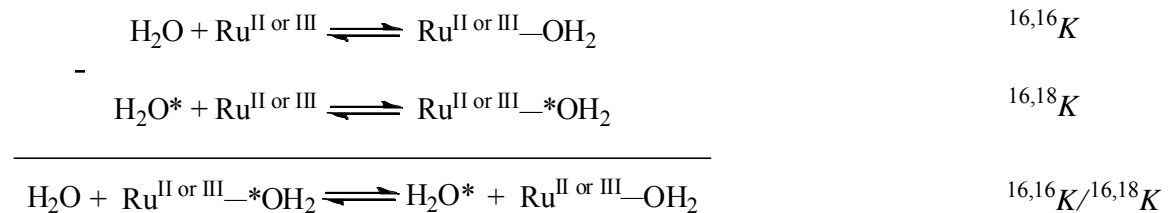


Scheme S4. Isotope exchange reactions for the reversible release of O₂ (a) and H₂O binding (b).

(a)



(b)



In the latter case the vibrational product (*VP*) was derived from the *MMI* partition function by removing the imaginary mode corresponding to the reaction coordinate frequency referred to throughout as ν_{RC} . The complete set of vibrational frequencies was implemented for the initial (A) and final (B) states per the Redlich-Teller product rule, using the generic isotope exchange equation A + B* → A* + B, where the asterisk designated the site of the heavy isotope. A is the initial reactant in all cases containing 3*N*-6 modes, where *N* is the number of atoms. B may be

the product with $3N-6$ stable modes or the transition state (TS) with $3N-7$ stable modes. The product with $3N-6$ vibrations was used to calculate ^{18}O EIEs whereas the TS with $3N-7$ vibrations was used to compute the ^{18}O KIEs defined by the expression below, where additional terms include h (Planck's constant), k (Boltzmann's constant) and T is temperature.

$$(S-1) \quad ^{18}\text{O} \text{ EIE} = ZPE \times EXC \times MMI$$

$$(S-2) \quad ZPE = \frac{\left[\prod_j^{3N-6} \frac{\exp(hv_j^{B*}/(2kT))}{\exp(hv_j^B/(2kT))} \right]}{\left[\prod_i^{3N-6} \frac{\exp(hv_i^{A*}/(2kT))}{\exp(hv_i^A/(2kT))} \right]}$$

$$(S-3) \quad EXC = \frac{\left[\prod_j^{3N-6} \frac{1 - \exp\{-(hv_j^{B*}/(kT))\}}{1 - \exp\{-(hv_j^B/(kT))\}} \right]}{\left[\prod_i^{3N-6} \frac{1 - \exp\{-(hv_i^{A*}/(kT))\}}{1 - \exp\{-(hv_i^A/(kT))\}} \right]}$$

$$(S-4) \quad MMI = \frac{\prod_j^{3N-6} (v_j^B / v_j^{B*})}{\prod_i^{3N-6} (v_i^A / v_i^{A*})}$$

The kinetic isotope effect is computed similarly using the terms described above, except that a pseudo-equilibrium constant for attaining the TS from the reactant is used. This term, ${}^{18}K_{\text{TS}}$, is defined as the product: $ZPE \times EXC \times VP$. In addition, the ${}^{18}\nu_{\text{RC}}$ is the ratio of the imaginary mode for the light TS isotopologue to the heavy TS isotopologue, or to the average of the two heavy isotopologues (vide infra). As a result, this term is invariably calculated to be ≥ 1 .

$$(S-5) \quad {}^{18}\text{O KIE} = ({}^{18}\nu_{\text{RC}})(ZPE \times EXC \times VP)$$

$$(S-6) \quad ZPE = \frac{\left[\prod_j^{{}^{3N-7}} \frac{\exp(hv_j^{B*}/(2kT))}{\exp(hv_j^B/(2kT))} \right]}{\left[\prod_i^{{}^{3N-6}} \frac{\exp(hv_i^{A*}/(2kT))}{\exp(hv_i^A/(2kT))} \right]}$$

$$(S-7) \quad EXC = \frac{\left[\prod_j^{{}^{3N-7}} \frac{1 - \exp\{-(hv_j^{B*}/(kT))\}}{1 - \exp\{-(hv_j^B/(kT))\}} \right]}{\left[\prod_i^{{}^{3N-6}} \frac{1 - \exp\{-(hv_i^{A*}/(kT))\}}{1 - \exp\{-(hv_i^A/(kT))\}} \right]}$$

$$(S-8) \quad VP = \frac{\prod_j^{{}^{3N-7}} (v_j^B / v_j^{B*})}{\prod_i^{{}^{3N-6}} (v_i^A / v_i^{A*})}$$

The isotope exchange reactions used to define the relevant ^{18}O KIEs and ^{18}O EIEs are provided in the accompanying text. The preference of heavy oxygen for the position associated with the weaker force constant and light oxygen for the stiffer force constant was considered by Boltzmann-weighting. Results are essentially equivalent to statistical averaging as shown below.

mPW91

Ru, WA ^{4a}	Ru=O + H ₂ O*	Ru=O* + H ₂ O
ZPE	0.9207	1.0274
MMI	1.1494	0.9826
EXC	0.9353	1.0099
$^{18}K_{\text{TS}}$	0.9898	1.0194
$^{18}v_{\text{RC}}$	1.0193	1.0204
^{18}KIE	1.0089	1.0402

Average $^{18}k_{\text{WA}} = 1.0246$

M06-L

Ru, WA ^{4a}	Ru=O + H ₂ O*	Ru=O* + H ₂ O
ZPE	0.9277	1.0355
MMI	1.1500	0.9821
EXC	0.9327	1.0094
$^{18}K_{\text{TS}}$	0.9950	1.0265
$^{18}v_{\text{RC}}$	1.0186	1.0209
^{18}KIE	1.0136	1.0480

Average $^{18}k_{\text{WA}} = 1.0308$

*m*PW91

$\text{Ru}_2^{\text{BD}} \text{WA}^2$	$[\text{Ru}^{\text{V}}=\text{O}, \text{Ru}^{\text{V}}=\text{O}] + \text{H}_2\text{O}^*$	$[\text{Ru}^{\text{V}}=\text{O}^*, \text{Ru}^{\text{V}}=\text{O}] + \text{H}_2\text{O}$
ZPE	0.9260	1.0172
MMI	1.1592	0.9859
EXC	0.9226	1.0100
$^{18}\text{K}_{\text{TS}}$	0.9903	1.0129
$^{18}\text{v}_{\text{RC}}$	1.0127	1.0147
^{18}KIE	1.0029	1.0278

Average $^{18}\text{k}_{\text{WA}} = 1.0154$

M06-L

$\text{Ru}_2^{\text{BD}} \text{WA}^2$	$[\text{Ru}^{\text{V}}=\text{O}, \text{Ru}^{\text{V}}=\text{O}] + \text{H}_2\text{O}^*$	$[\text{Ru}^{\text{V}}=\text{O}^*, \text{Ru}^{\text{V}}=\text{O}] + \text{H}_2\text{O}$
ZPE	0.9229	1.0254
MMI	1.1585	0.9867
EXC	0.9248	1.0074
EIE	0.9888	1.0193
$^{18}\text{v}_{\text{RC}}$	1.0132	1.0140
^{18}KIE	1.0019	1.0336

Average $^{18}\text{k}_{\text{WA}} = 1.0178$

Table S-1. Reduced partition function calculation of ^{18}O KIE(O–O) for **Ru**.

Ru	$^{18}\nu_{\text{RC}}$ <i>mPW91 / M06-L</i>	ZPE <i>mPW91 / M06-L</i>	VP <i>mPW91 / M06-L</i>	EXC <i>mPW91 / M06-L</i>	$^{18}K_{\text{TS}}$ <i>mPW91 / M06-L</i>	$^{16,18}\nu_{\text{RC}} (\text{cm}^{-1})$ <i>mPW91 / M06-L</i>
$^2\text{WA}^{4a}$	1.0198/ 1.0197	0.9703/ 0.9779	1.0605/ 1.0604	0.9706/ 0.9690	1.0041/ 1.0103	-263.77/ -411.61
$^2\text{WA}^{4a}$ (SMD)	1.0221/ n.d.	0.9779/ n.d.	1.0549/ n.d.	0.9700/ n.d.	1.0054/ n.d.	-227.63/ n.d.
$^2\text{WA}^{4b}$	n.d./ 1.0092	n.d./ 0.9758	n.d./ 1.0703	n.d./ 0.9593	n.d./ 1.0064	n.d./ -307.92
$^2\text{WA}^{4b}$ (SMD)	n.d./ 1.0123	n.d./ 0.9896	n.d./ 1.0633	n.d./ 0.9573	n.d./ 1.0113	n.d./ -465.92
$^2\text{WA}^5$	1.0085/ 1.0078	0.9665/ 0.9698	1.0729/ 1.0709	0.9617/ 0.9616	1.0021/ 1.0034	-561.74/ -327.32

Table S-2. Reduced partition function calculation of ^{18}O KIE(O–O) for Ru_2^{BD} .

Ru_2^{BD}	$^{18}\nu_{\text{RC}}$ $m\text{PW91} /$ M06-L	ZPE $m\text{PW91} /$ M06-L	VP $m\text{PW91} /$ M06-L	EXC $m\text{PW91} /$ M06-L	$^{18}K_{\text{TS}}$ $m\text{PW91} /$ M06-L	$^{16,18}\nu \text{ (cm}^{-1}\text{)}$ $m\text{PW91} /$ M06-L
$^1\text{WA}^1$	1.0057/	0.9553/	1.0751/	0.9641/	0.9954/	-923.30/
	1.0072	0.9627	1.0731	0.9632	0.9998	-958.40
$^1\text{WA}^1$ (SMD)	1.0060/	0.9611/	1.0747/	0.9614/	0.9985/	-888.12/
	1.0039	0.9564	1.0783	0.9607	0.9953	-1144.66
$^3\text{WA}^1$	n.d./	n.d./	n.d./	n.d./	n.d./	n.d./
	1.0043	0.9561	1.0760	0.9638	0.9964	-1096.87
$^5\text{WA}^1$	n.d./	n.d./	n.d./	n.d./	n.d./	n.d./
	1.0113	0.9687	1.0676	0.9633	1.0007	-715.23
$^1\text{WA}^2$	1.0137/	0.9688/	1.0667/	0.9637/	1.0013/	-572.34/
	1.0135	0.9706	1.0670	0.9637	1.0036	-571.78
$^1\text{WA}^2$ (SMD)	1.0218/	0.9711/	1.0581/	0.9680/	1.0004/	-426.85/
	1.0118	0.9580	1.0724	0.9658	0.9977	-578.11
$^3\text{WA}^2$	n.d./	n.d./	n.d./	n.d./	n.d./	n.d./

	1.0110	0.9711	1.0691	0.9614	1.0035	-617.03
⁵ WA ²	n.d./ 1.0166	n.d./ 0.9712	n.d./ 1.0633	n.d./ 0.9646	n.d./ 1.0020	n.d./ -504.46
¹ OC	n.d./ 1.0223	n.d./ 1.0238	n.d./ 0.9792	n.d./ 1.0138	n.d./ 1.0165	n.d./ -345.78
³ OC	n.d./ 1.0294	n.d./ 1.0218	n.d./ 0.9714	n.d./ 1.0192	n.d./ 1.0117	n.d./ -318.99
⁵ OC	n.d./ 1.0278	n.d./ 1.0294	n.d./ 0.9731	n.d./ 1.0147	n.d./ 1.0166	n.d./ -343.84

Table S-3. Reduced partition function calculation of ¹⁸O KIE(O–O) for Ru₂^{Hbpp}.

Ru ₂ ^{Hbpp}	¹⁸ v _{RC} <i>mPW91</i> / M06-L	ZPE <i>mPW91</i> / M06-L	VP <i>mPW91</i> / M06-L	EXC <i>mPW91</i> / M06-L	¹⁸ K _{TS} <i>mPW91</i> / M06-L	^{16,18} v _{RC} (cm ⁻¹) <i>mPW91</i> / M06-L
¹ WA ¹ (IV,IV)	1.0061/ 1.0008	0.9543/ 0.9571	1.0748/ 1.0796	0.9638/ 0.9608	0.9934/ 0.9978	-693.15/ -1436.73

¹WA² (IV,IV)	1.0012/ 1.0010	0.9654/ 0.9700	1.0793/ 1.0794	0.9556/ 0.9535	1.0006/ 1.0034	-1152.41/ -1412.46
¹OC (IV,IV)	1.0203/ 1.0281	1.0170/ 1.0248	0.9800/ 0.9729	1.0137/ 1.0189	1.0104/ 1.0160	-156.96/ -396.84
¹OC (IV,IV) (SMD)	n.d./ 1.0282	n.d./ 1.0286	n.d./ 0.9733	n.d./ 1.0170	n.d./ 1.0182	n.d./ -384.84
²WA¹ (IV,V)	1.0189/ 1.0227	0.9762/ 0.9852	1.0608/ 1.0566	0.9660/ 0.9680	1.0044/ 1.0113	-376.22/ -228.49
²WA² (IV,V)	1.0155/ 1.0110	0.9811/ 0.9847	1.0643/ 1.0693	0.9613/ 0.9564	1.0083/ 1.0121	-141.56/ -437.39
²OC (IV,V)	n.d./ 1.0272	n.d./ 1.0238	n.d./ 0.9736	n.d./ 1.0200	n.d./ 1.0167	n.d./ -337.18
⁴WA¹ (IV,V)	1.0197/ 1.0230	0.9779/ 0.9852	1.0599/ 1.0565	0.9666/ 0.9674	1.0061/ 1.0108	-382.20/ -248.36
⁴WA² (IV,V)	1.0167/ 1.0113	0.9831/ 0.9865	1.0631/ 1.0689	0.9619/ 0.9556	1.0099/ 1.01283	-146.26/ -430.98

⁴OC (IV,V)	1.0264/	1.0239/	0.9744/	1.0180/	1.0157/	-277.64/
	1.0279	1.0321	0.9730	1.0172	1.0216	-408.76
⁴OC (IV, V) (SMD)	1.0244/	1.0273/	0.9757/	1.0116/	1.0141/	-242.03/
	1.0274	1.0287	0.9735	1.0167	1.0183	-421.28

Calculated Vibrational Frequencies of Water

H₂O (mPW91)

D₂O (mPW91)

16	18		16	18
1672.893	1665.824		1225.14	1216.288
3647.852	3640.434		2628.01	2617.323
3773.26	3757.823		2765.147	2744.038

H₂O (M06-L)

D₂O (M06-L)

16	18		16	18
1746.834	1739.676		1277.87	1268.939
3797.261	3789.053		2738.7	2726.904

3937.48	3921.641		2883.824	2862.159
---------	----------	--	----------	----------

H₂O (SMD) (mPW91) **H₂O (SMD) (M06-L)**

16	18		16	18
1640.039	1633.301		1695.674	1688.906
3645.037	3637.198		3775.161	3766.597
3741.44	3726.248		3883.54	3868.098

Table S-4. Reduced partition function calculation of ¹⁸O KIE(H₂O) for **Ru**.

Ru	¹⁸ v _{RC} mPW/M06-L	ZPE mPW/M06-L	VP mPW/M06-L	EXC mPW/M06-L	¹⁸ K _{TS} mPW/M06-L
² Ru, WA ^{4a}	1.0199/ 1.0196	0.9318/ 0.9351	1.1497/ 1.150	0.9359/ 0.9359	1.0026/ 1.0062
² Ru, WA ^{4a} (SMD)	1.0221/ n.d.	0.9326/ n.d.	1.1475/ n.d.	0.9358/ n.d.	1.0015/ n.d.
² Ru, WA ^{4b}	n.d./ 1.0092	n.d./ 0.9310	n.d./ 1.1619	n.d./ 0.9262	n.d./ 1.0022

²Ru, WA^{4b} (SMD)	n.d./ 1.0123	n.d. /0.9416	n.d./ 1.1564	n.d./ 0.9249	n.d./ 1.0067
²Ru, WA⁵	1.0085/ 1.0078	0.9275/ 0.9256	1.1635/ 1.1624	0.9272/ 0.9285	1.0006/ 0.9992

Table S-5. Reduced partition function calculation of ¹⁸O KIE(H₂O) for **Ru₂^{BD}**.

Ru ₂ ^{BD}	¹⁸ v _{RC} <i>mPW/M06-L</i>	ZPE <i>mPW/ M06-L</i>	VP <i>mPW / M06-L</i>	EXC <i>mPW/M06-L</i>	¹⁸ K _{TS} <i>mPW/M06-L</i>
¹Ru₂^{BD}, WA¹	1.0057/ 1.0072	0.9181/ 0.9220	1.1685/ 1.1668	0.9294/ 0.9293	0.9971/ 0.9996
¹Ru₂^{BD}, WA¹(SMD)	1.0059/ 1.0039	0.9248/ 0.9218	1.1678/ 1.1706	0.9266/ 0.9253	1.0007/ 0.9979
³Ru₂^{BD}, WA¹	n.d./ 1.0043	n.d./ 0.9166	n.d./ 1.1706	n.d./ 0.9300	n.d./ 0.9977
⁵Ru₂^{BD}, WA¹	n.d./ 1.0113	n.d./ 0.9286	n.d./ 1.1617	n.d./ 0.9288	n.d./ 1.0018

¹ Ru ₂ ^{BD} , WA ²	1.0135/ 1.0134	0.9316/ 0.9309	1.1588/ 1.1589	0.9292/ 0.9303	1.0032/ 1.0036
¹ Ru ₂ ^{BD} , WA ² (SMD)	1.0215/ 1.0115	0.9352/ 0.9251	1.1492/ 1.1618	0.9330/ 0.9305	1.0027/ 1.0001
³ Ru ₂ ^{BD} , WA ²	n.d./ 1.0108	n.d./ 0.9319	n.d./ 1.1619	n.d./ 0.9281	n.d./ 1.0050
⁵ Ru ₂ ^{BD} , WA ²	n.d./ 1.0163	n.d./ 0.9327	n.d./ 1.1554	n.d./ 0.9310	n.d./ 1.0033
¹ Ru ₂ ^{BD} , OC	n.d./ 1.0223	n.d./ 0.9377	n.d./ 1.1506	n.d./ 0.9419	n.d./ 1.0162
³ Ru ₂ ^{BD} , OC	n.d./ 1.0295	n.d./ 0.9375	n.d./ 1.1426	n.d./ 0.9470	n.d./ 1.0144
⁵ Ru ₂ ^{BD} , OC	n.d./ 1.0279	n.d./ 0.9449	n.d./ 1.1445	n.d./ 0.9418	n.d./ 1.0185

Table S-6. Reduced partition function calculation of ^{18}O KIE(H_2O) for $\text{Ru}_2^{\text{Hbpp}}$.

$\text{Ru}_2^{\text{Hbpp}}$	$^{18}\nu_{\text{RC}}$ <i>mPW/M06-L</i>	ZPE <i>mPW/ M06-L</i>	VP <i>mPW / M06-L</i>	<i>EXC</i> <i>mPW/M06-L</i>	$^{18}K_{\text{TS}}$ <i>mPW/M06-L</i>
$^1\text{WA}^1 \text{(IV,IV)}$	1.0061/ 1.0008	0.9217/ 0.9213	1.1693/ 1.1750	0.9264/ 0.9242	0.9985/ 1.0006
$^1\text{WA}^2 \text{(IV,IV)}$	1.0013/ 1.0011	0.9322/ 0.9335	1.1744/ 1.1748	0.9186/ 0.9172	1.0058/ 1.0062
$^1\text{OC (IV,IV)}$	1.0204/ 1.0282	0.9446/ 0.9491	1.1534/ 1.1448	0.9340/ 0.9403	1.1767/ 1.0216
$^1\text{OC (IV,IV)}$ (SMD)	n.d./ 1.0282	n.d./ 0.9513	n.d./ 1.1446	n.d./ 0.9400	n.d./ 1.0235
$^2\text{WA}^1 \text{(IV,V)}$	1.0189/ 1.0227	0.9435/ 0.9470	1.1544/ 1.1502	0.9274/ 0.9299	1.0102/ 1.0131
$^2\text{WA}^2 \text{(IV,V)}$	1.0156/ 1.0110	0.9486/ 0.9476	1.1579/ 1.1633	0.9233/ 0.9196	1.0141/ 1.0139
$^2\text{OC (IV,V)}$	n.d./	n.d./	n.d./	n.d./	n.d./

	1.0273	0.9468	1.1458	0.9404	1.0202
⁴ WA ¹ (IV,V)	1.0198/	0.9440/	1.1535/	0.9280/	1.0105/
	1.0231	0.9457	1.1500	0.9303	1.0119
⁴ WA ² (IV,V)	1.0168/	0.9493/	1.1566/	0.9238/	1.0144/
	1.0114	0.9480	1.1628	0.9197	1.0139
⁴ OC (IV,V)	1.0264/	0.9508/	1.1468/	0.9368/	1.0215/
	1.0280	0.9516	1.1451	0.9396	1.0238
⁴ OC (IV, V) (SMD)	1.0244/	0.9536/	1.1482/	0.9329/	1.0214/
	1.0275	0.9509	1.1457	0.9386	1.0226

Additional Computational Details

¹⁸O KIEs are calculated for **OC** and **WA** mechanisms occurring during catalytic water oxidation by considering all microscopic steps, beginning with H₂O coordination to the reduced ruthenium species, leading up to and including the O–O bond formation step. Expressions for the isotope effect, KIE(H₂O), corresponding to Eq 6 where all steps are reversible prior to O–O bond formation, are presented in the tables below. The results are compared to the ¹⁸O KIE(O–O) which represents the ¹⁸O KIE on the microscopic step for O–O bond formation.

Aqueous free energies of activation were computed in two ways following geometry optimization. In the first approach, aqueous solvation free energies computed from the SMD

continuum solvation model were added to the gas-phase free energies computed at the *m*PW or M06-L levels detailed above. In the second approach, thermal contributions from the level employed for geometry optimization were added to single-point M06-L electronic energies computed with the SDD basis set for ruthenium and the 6-311+G(2df,p) basis for all other atoms. Calculations reflect a 1 M standard state for the ruthenium complexes in aqueous solution. Water is present at its bulk concentration of 55.6 M. For all molecules except water, free energies in solution were computed including a 1 atm to 1 M standard-state concentration change (1.9 kcal mol⁻¹) in addition to the 1 M to 1 M (solvation) transfer free energy computed from the SMD model. In the case of water, a 1 atm to 55.6 M standard-state concentration change (4.3 kcal mol⁻¹) is added to the 1 M to 1 M experimental solvation free energy (-6.3 kcal mol⁻¹).]

Table S-7. Summary of DFT-calculated parameters for catalysis initiated by **Ru**.

TS ^a	$\Delta G^\ddagger(\text{O}-\text{O})$ ^b (kcal mol ⁻¹)	¹⁸ O KIE(O–O) ^c <i>m</i> PW / M06-L	¹⁸ O KIE(H ₂ O) ^d <i>m</i> PW / M06-L
² Ru, WA ^{4a}	22.5	1.0240 / 1.0303	1.0225 / 1.0260
² Ru, WA ^{4a} (SMD)	23.1 ^e	1.0277 / —	1.0236 / —
² Ru, WA ^{4b}	19.0	— / 1.0158	— / 1.0114
² Ru, WA ^{4b} (SMD)	20.0 ^e	— / 1.0237	— / 1.0191
² Ru, WA ⁵	20.6	1.0106 / 1.0113	1.0090 / 1.0070

^a Attained from the doublet, ²Ru^V=O, precursor. ^b Single-point corrected for spin and solvation unless noted. ^c Calculated for the microscopic O–O bond formation step. ^d Calculated for reversible steps beginning with H₂O coordination and leading up to irreversible O–O bond formation. ^e Computed from structures re-optimized including SMD aqueous solvation effects.

Table S-8. Summary of DFT-calculated parameters for catalysis initiated by **Ru₂^{BD}**.

TS	$\Delta G^\ddagger(\text{O–O})$ (kcal mol ⁻¹) ^{c,d}	¹⁸ OKIE (O–O) <i>m</i> PW / M06-L ^d	¹⁸ O KIE (H ₂ O) <i>m</i> PW / M06-L ^e
¹ Ru ₂ ^{BD} , WA ¹ (SMD) ^a	54.0 ^f	1.0046 / 0.9993	1.0066 / 1.0018
¹ Ru ₂ ^{BD} , WA ¹ ^a	46.8	1.0012 / 1.0071	1.0028 / 1.0068
³ Ru ₂ ^{BD} , WA ¹ ^b	31.3	— / 1.0007	— / 1.0020
⁵ Ru ₂ ^{BD} , WA ¹ ^b	28.9	— / 1.0121	1.0050 / 1.0130
¹ Ru ₂ ^{BD} , WA ² (SMD) ^a	34.4 ^f	1.0222 / 1.0095	1.0243 / 1.0120
¹ Ru ₂ ^{BD} , WA ² ^a	36.5	1.0151 / 1.0172	1.0167 / 1.0170
³ Ru ₂ ^{BD} , WA ² ^b	27.0	— / 1.0146	— / 1.0158
⁵ Ru ₂ ^{BD} , WA ² ^b	31.9	— / 1.0184	— / 1.0196
¹ Ru ₂ ^{BD} , OC ^a	27.3	— / 1.0393	— / 1.0389

³ Ru ₂ ^{BD} , OC ^b	10.0	— / 1.0416	— / 1.0443
⁵ Ru ₂ ^{BD} , OC ^b	7.8	— / 1.0449	— / 1.0469

^a Relative to the di-ruthenium (V, V) bis-oxo intermediate in an unrestricted singlet state, having a staggered conformation. ^b Relative to the corresponding di-ruthenium (V, V) bis-oxo intermediate in the triplet or quintet spin state, having an eclipsed conformation. ^c Calculated at the M06-L level using single-point corrections unless noted. ^d Calculated for the microscopic O–O bond formation step. ^e Calculated in a manner that includes all reversible steps, beginning with H₂O coordination and leading up to irreversible O–O bond formation. ^f Calculated using SMD at the M06-L level of theory.

Table S-9. Summary of DFT-calculated parameters for catalysis initiated by Ru₂^{Hbpp}.

TS ^a	ΔG [‡] (O–O) kcal mol ⁻¹ ^b	¹⁸ O KIE(O–O) ^c mPW / M06-L	¹⁸ O KIE(H ₂ O) ^d mPW / M06-L
¹ Ru ₂ ^{Hbpp} , WA ¹ (IV,IV)	43.9	0.9995 / 0.9987	1.0046 / 1.0014
¹ Ru ₂ ^{Hbpp} , WA ² (IV,IV)	55.9	1.0020 / 1.0046	1.0071 / 1.0073
¹ Ru ₂ ^{Hbpp} , OC (IV,IV) (SMD)	16.5 ^e	— / 1.0470	— / 1.0524
¹ Ru ₂ ^{Hbpp} , OC (IV,IV)	14.3	1.0311 / 1.0447	1.0385 / 1.0504
² Ru ₂ ^{Hbpp} , WA ¹ (IV,V)	27.4	1.0235 / 1.0344	1.0294 / 1.0360

² Ru ₂ ^{Hbpp} , WA ² (IV,V)	27.6	1.0241 / 1.0234	1.0299 / 1.0250
² Ru ₂ ^{Hbpp} , OC (IV,V)	13.8	— / 1.0445	— / 1.0480
⁴ Ru ₂ ^{Hbpp} , WA ¹ (IV,V)	27.4	1.0260 / 1.0342	1.0305 / 1.0353
⁴ Ru ₂ ^{Hbpp} , WA ² (IV,V)	26.7	1.0269 / 1.0244	1.0314 / 1.0254
⁴ Ru ₂ ^{Hbpp} , OC (IV, V) (SMD)	12.5 ^e	1.0389 / 1.0463	1.0463 / 1.0506
⁴ Ru ₂ ^{Hbpp} , OC (IV,V)	11.4	1.0426 / 1.0503	1.0485 / 1.0524

^a Relative to the di-ruthenium bis oxo precursor in the oxidation states indicated in the gas phase or aqueous dielectric continuum model. ^b Calculated at the M06-L level of theory or using single-point corrections as described in the Experimental. ^c Calculated for the microscopic O–O bond formation step. ^d Calculated assuming reversible steps beginning with H₂O coordination leading up to O–O bond formation in the first irreversible step. ^e Calculated using SMD at the M06-L level of theory.

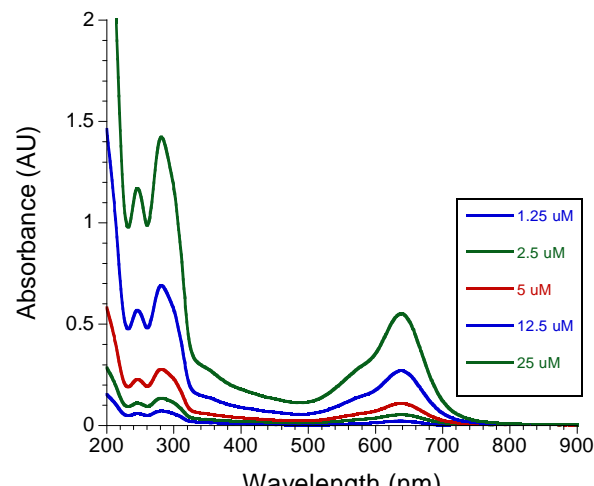
Table S-10. Comparison of gas phase ¹⁸O KIE(H₂O) and ¹⁸O KIE(D₂O). Contributions from the isotope effects on the reaction coordinate frequency are given in parentheses.

mPW91	Proposed TS	¹⁸ O KIE _{calc} H ₂ O (¹⁸ v _{RC})	¹⁸ O KIE _{calc} D ₂ O(¹⁸ v _{RC})
Ru	WA ^{4a}	1.0242 (1.0199)	1.0275 (1.0179)
Ru ₂ ^{BD}	WA ²	1.0151 (1.0137)	1.0210 (1.0138)

M06-L	Proposed TS	^{18}O KIE _{calc} H ₂ O ($^{18}\text{v}_{\text{RC}}$)	^{18}O KIE _{calc} D ₂ O($^{18}\text{v}_{\text{RC}}$)
Ru	WA ^{4a}	1.0303 (1.0198)	1.0355 (1.0188)
Ru_2^{BD}	WA ²	1.0172 (1.0073)	1.0235 (1.0136)

Figure S-1: UV-Vis spectra (a) and Beer's Law plot (b) for Ru_2^{BD} : $\epsilon_{638 \text{ nm}} = 22000 \text{ M}^{-1}\text{cm}^{-1}$, $\epsilon_{281 \text{ nm}} = 56500 \text{ M}^{-1}\text{cm}^{-1}$ and $\epsilon_{638 \text{ nm}} = 46500 \text{ M}^{-1}\text{cm}^{-1}$. Purity based on $\epsilon_{638 \text{ nm}} = 100 \pm 1 \%$.

a.



b.

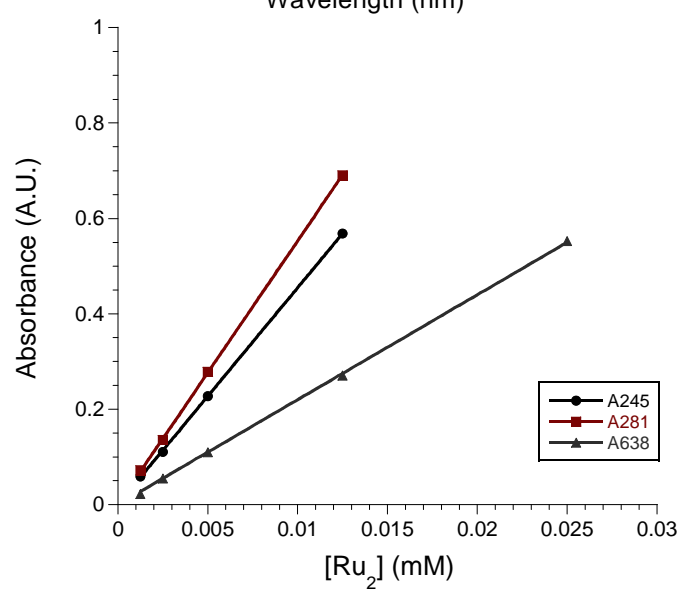


Figure S-2: Quantitative ^1H NMR spectrum of Ru_2^{BD} (2.5×10^{-5} moles) and HMDS (4.2×10^{-6} moles) in d_6 -DMSO (purity based on internal standard = $105 \pm 6\%$).

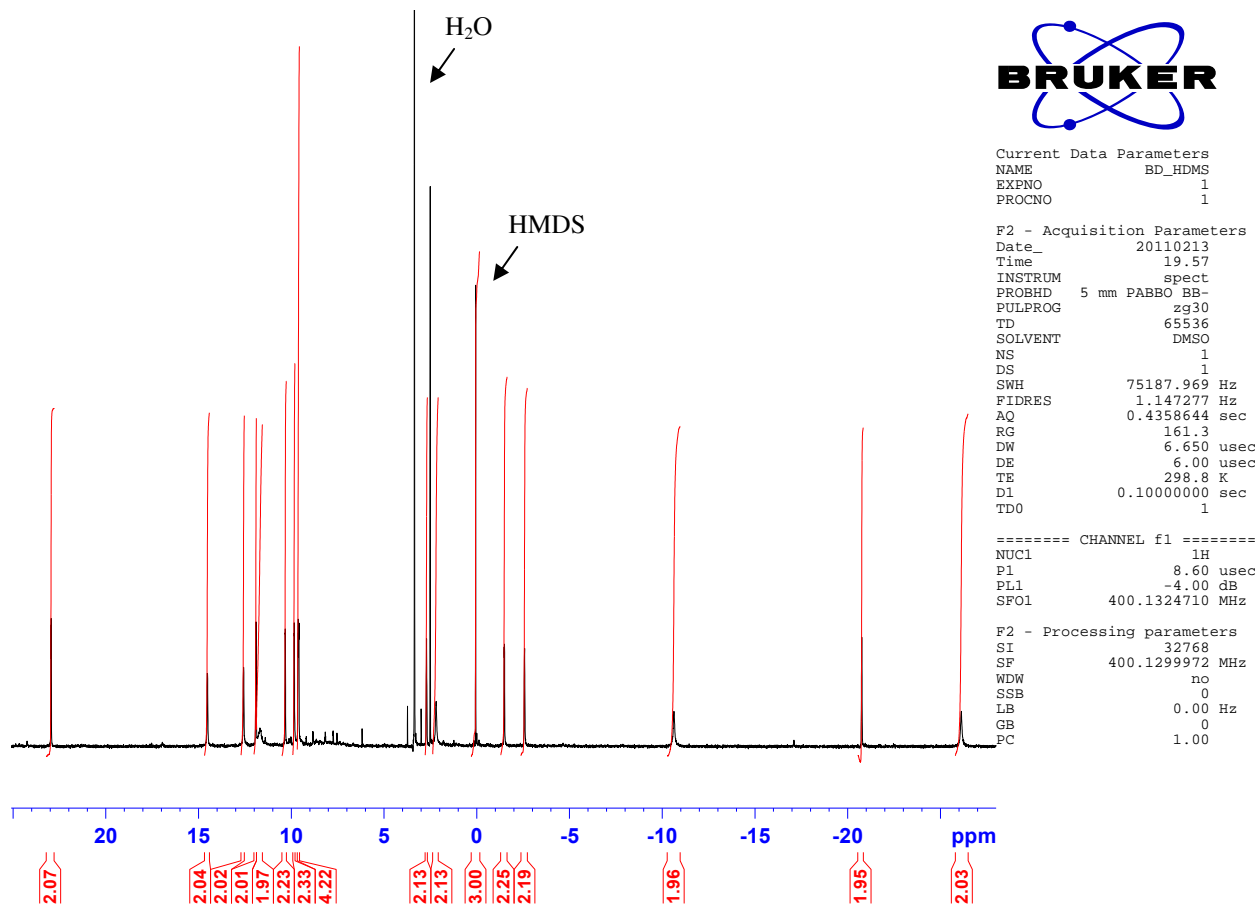


Figure S-3: Expanded views of the spectrum in Figure S-2

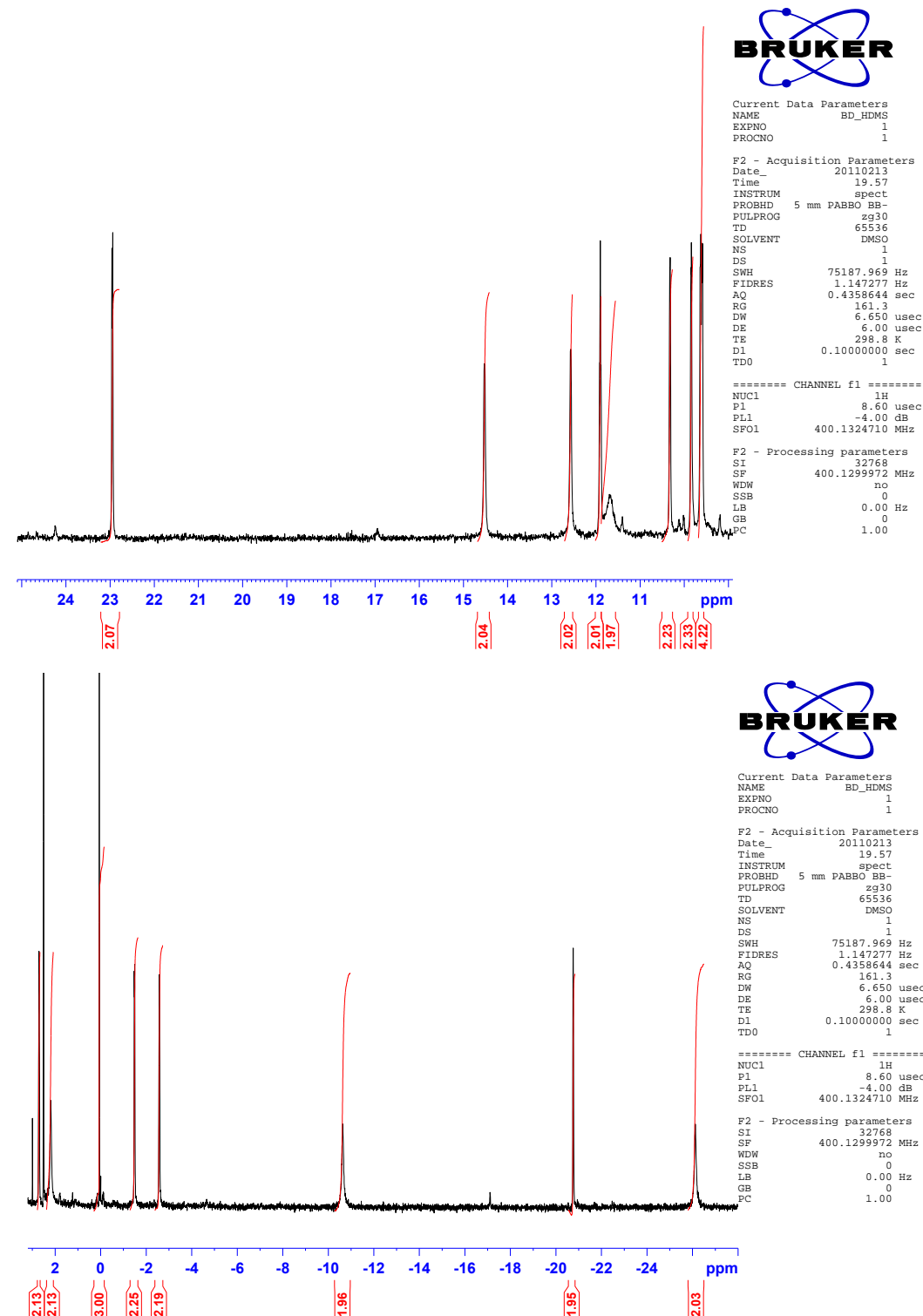
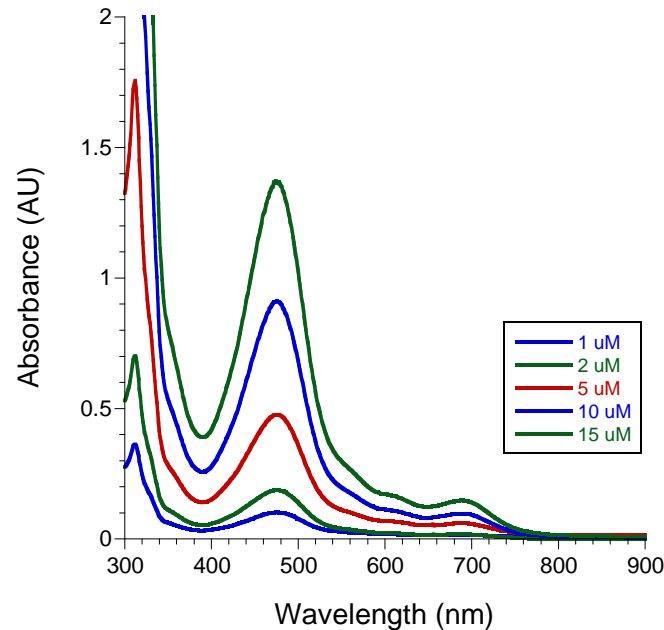


Figure S-4: UV-Vis spectra (a) and Beer's Law plot (b) for Ru: $\epsilon_{475\text{nm}} = 9200 \text{ M}^{-1}\text{cm}^{-1}$. The purity is estimated to be $96 \pm 1 \%$ based on $\epsilon_{475\text{ nm}}$ ($9600 \text{ M}^{-1} \text{ cm}^{-1}$).

a.



b.

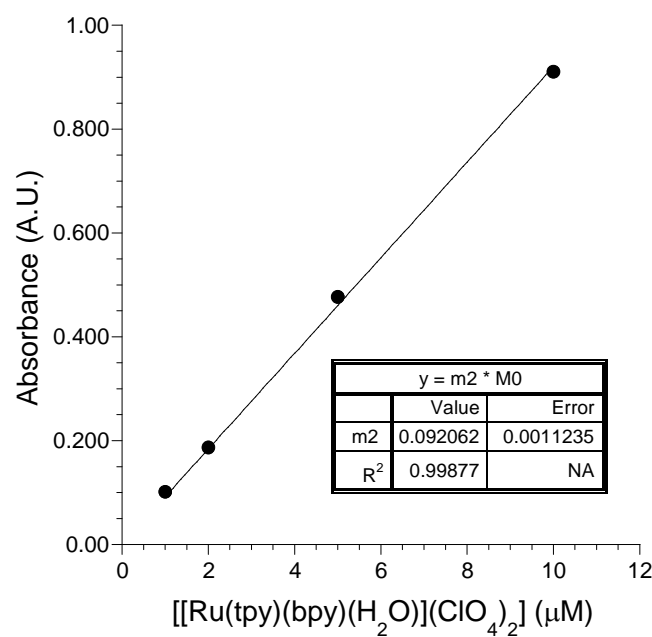


Figure S-5: Quantitative ^1H NMR spectrum of **Ru** (1.3×10^{-5} moles) and HMDS (1.2×10^{-5} moles) in CD_3OD (purity based on internal standard $99 \pm 6\%$).

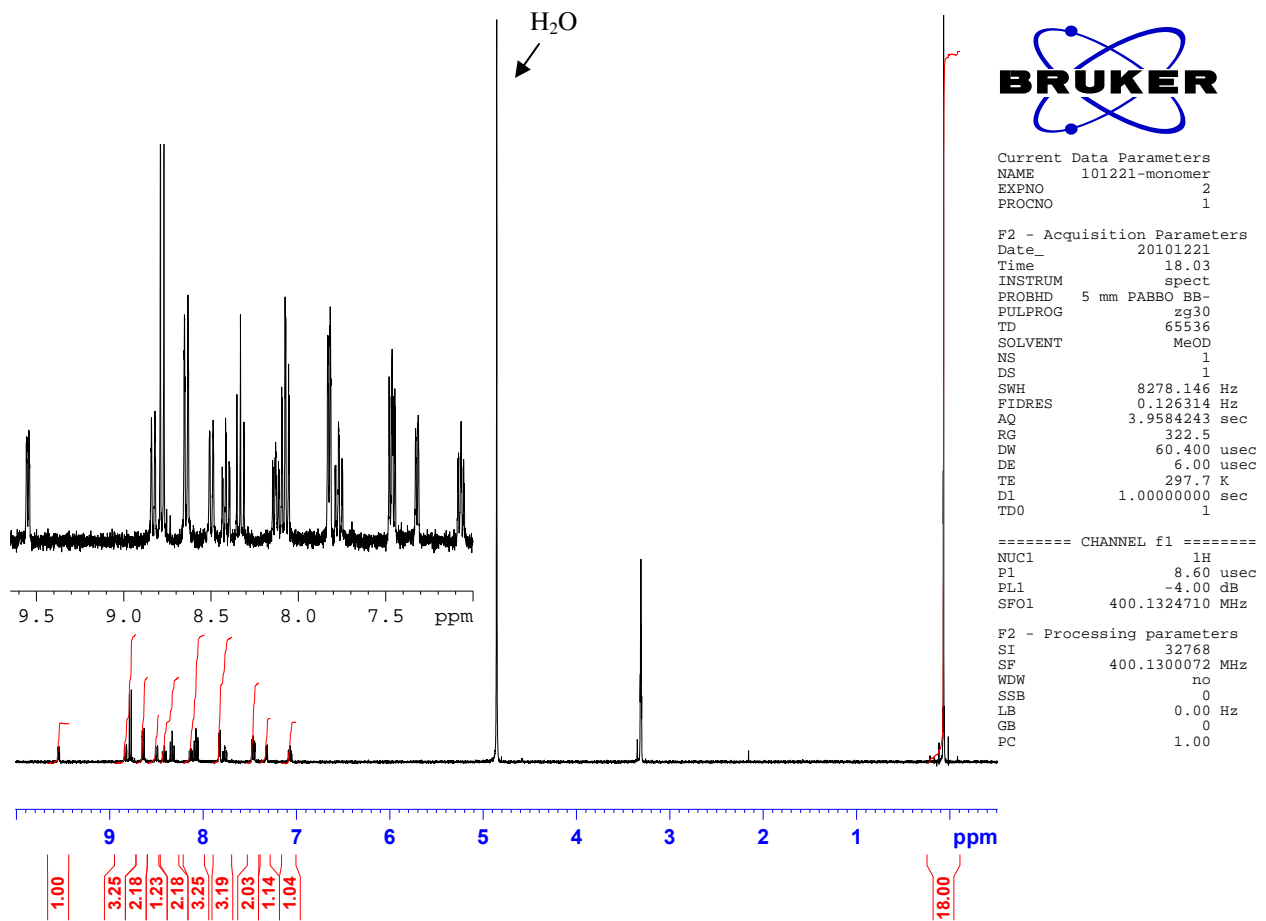


Figure S-6: UV-Vis spectra (a) and Beer's Law plot (b) for $\text{Ru}_2^{\text{HbPP}}$: $\epsilon_{471\text{nm}} = 11320 \text{ M}^{-1}\text{cm}^{-1}$.

The purity is estimated to be $95 \pm 1 \%$ based on the $\epsilon_{471\text{nm}}$ ($11880 \text{ M}^{-1}\text{cm}^{-1}$).

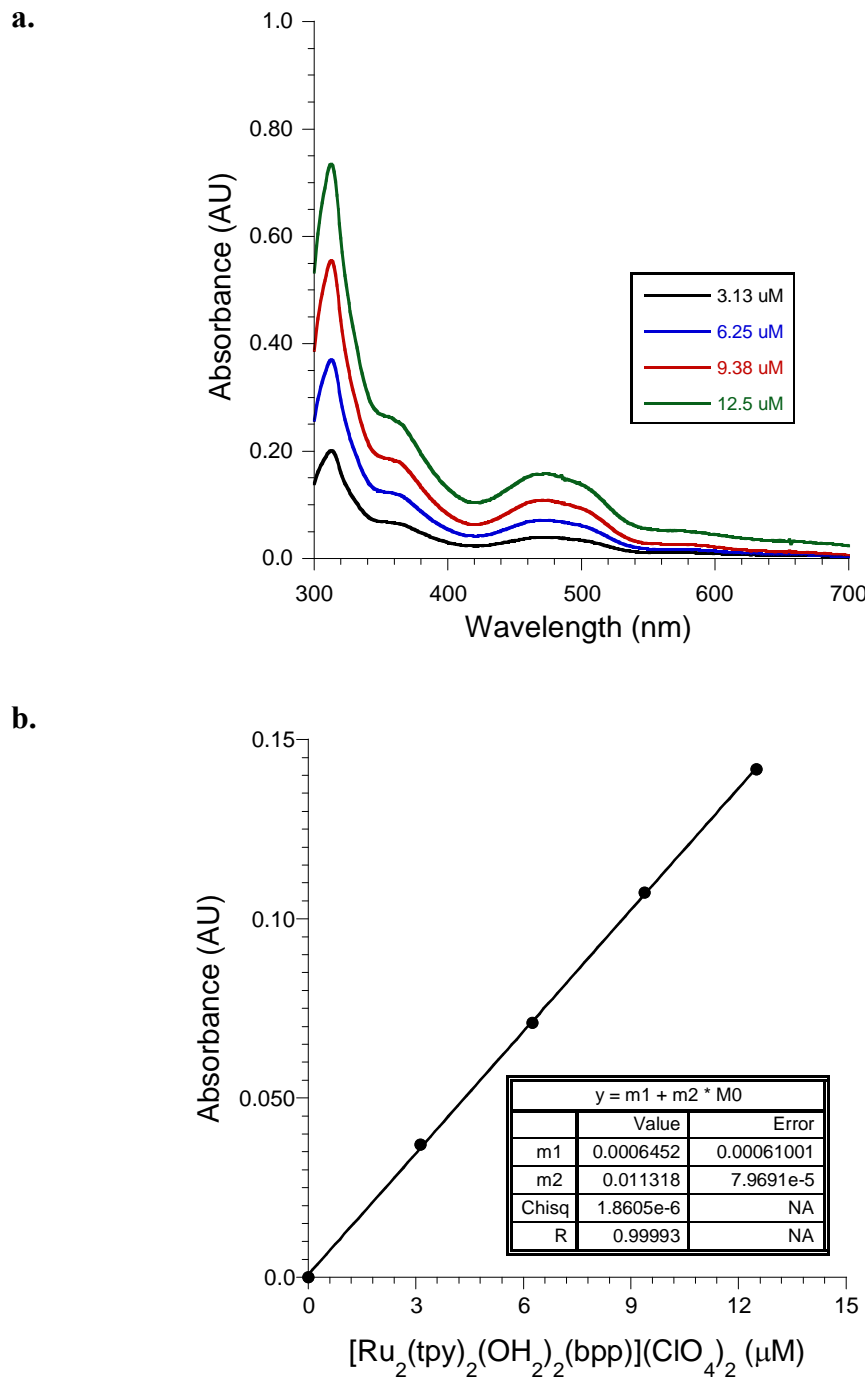


Figure S-7: Quantitative ^1H NMR spectrum of $\text{Ru}_2^{\text{Hbpp}}$ (1.15×10^{-5} moles) and HMDS (1.25×10^{-5} moles) in acetone-d₆ (purity based on internal standard $100 \pm 5\%$).

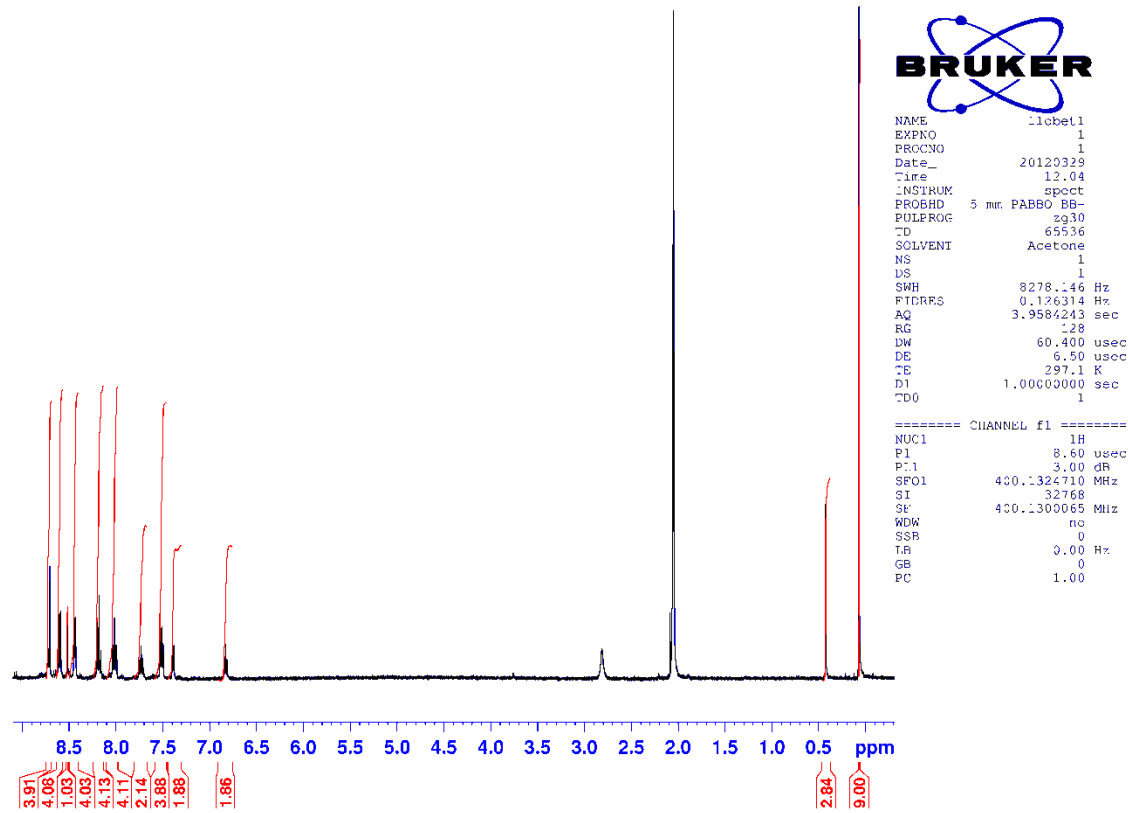
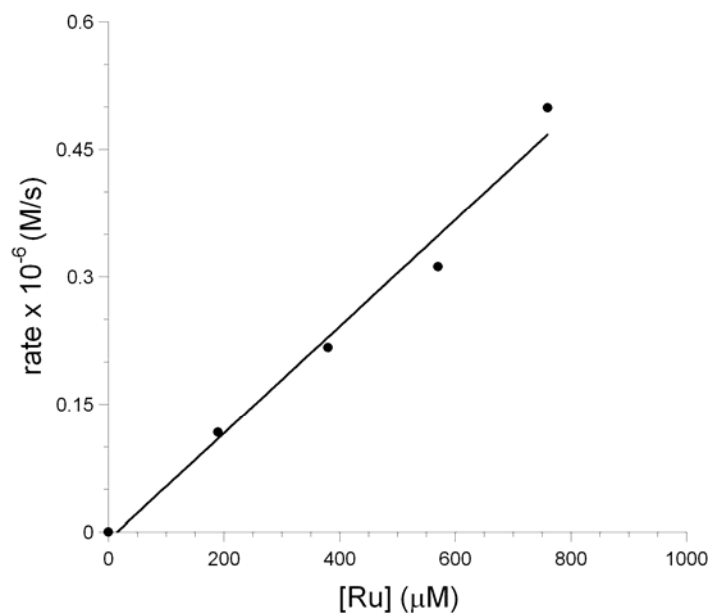


Figure S-8: Plots of initial rate versus \mathbf{Ru} (a), $\mathbf{Ru}_2^{\text{BD}}$ (b) and $\mathbf{Ru}_2^{\text{HbPP}}$ (c) measured using a YSI O_2 electrode as described in the text.

(a)



(b)

